World Journal of Radiology

Submit a Manuscript: http://www.wjgnet.com/esps/
Help Desk: http://www.wjgnet.com/esps/helpdesk.aspx
DOI: 10.4329/wjr.v8.i2.174

World J Radiol 2016 February 28; 8(2): 174-182
ISSN 1949-8470 (online)

MINIREVIEWS

Benign neck masses showing restricted diffusion: Is there a histological basis for discordant behavior?

Abanti Das, Ashu S Bhalla, Raju Sharma, Atin Kumar, Meher Sharma, Shivanand Gamanagatti, Alok Thakar, Suresh Sharma

Abanti Das, Ashu S Bhalla, Raju Sharma, Atin Kumar, Shivanand Gamanagatti, Department of Radiodiagnosis, All India Institute of Medical Sciences, New Delhi 110029, India

Meher Sharma, Department of Pathology, All India Institute of Medical Sciences, New Delhi 110029, India

Alok Thakar, Suresh Sharma, Department of Otolaryngorhinology, All India Institute of Medical Sciences, New Delhi 110029, India

Author contributions: Das A, Bhalla AS, Sharma R and Kumar A contributed to study design and conception and writing the article; critically analyzing the scientific content and image preparation; Sharma M contributed to image preparation and reviewing the article; Gamanagatti S, Thakar A and Sharma S contributed to article preparation and approving the final version.

Conflict-of-interest statement: The authors declare no conflicts of interest regarding this manuscript.

Correspondence to: Ashu Seith Bhalla, Professor, Department of Radiodiagnosis, All India Institute of Medical Sciences, Ansari Nagar, New Delhi 110029, India. ashubhalla1@yahoo.com
Telephone: +91-011-26594925

Received: June 16, 2015
Peer-review started: June 17, 2015
First decision: August 22 2015
Revised: September 29, 2015
Accepted: December 18, 2015
Article in press: December 21, 2015
Published online: February 28, 2016

Abstract

Diffusion weighted imaging (DWI) evolved as a complementary tool to morphologic imaging by offering additional functional information about lesions. Although the technique utilizes movement of water molecules to characterize biological tissues in terms of their cellularity, there are other factors related to the histological constitution of lesions which can have a significant bearing on DWI. Benign lesions with atypical histology including presence of lymphoid stroma, inherently increased cellularity or abundant extracellular collagen can impede movement of water molecules similar to malignant tissues and thereby, show restricted diffusion. Knowledge of these atypical entities while interpreting DWI in clinical practice can avoid potential misdiagnosis. This review aims to present an imaging spectrum of such benign neck masses which, owing to their distinct histology, can show discordant behavior on DWI.

Key words: Diffusion weighted imaging; Benign neck masses; Restricted diffusion

Core tip: Diffusion weighted imaging improves lesion characterization by providing functional information. However, apart from tissue cellularity, histological background of the lesion can significantly influence the diffusion characteristics of the lesion. Consequently, even benign lesions with atypical histology can show restricted diffusion leading to potential errors in diagnosis.

Das A, Bhalla AS, Sharma R, Kumar A, Sharma M, Gamanagatti S, Thakar A, Sharma S. Benign neck masses showing restricted diffusion: Is there a histological basis for discordant behavior? *World J Radiol* 2016; 8(2): 174-182 Available from: URL: http://www.wjgnet.com/1949-8470/full/v8/i2/174.htm DOI: http://dx.doi.org/10.4329/wjr.v8.i2.174

INTRODUCTION

Diffusion weighted imaging (DWI) was introduced as an adjunct to conventional magnetic resonance imaging (MRI) to enable better characterization of biological tissues. This MR technique interrogates diffusivity of water molecules in tissues and the functional information obtained can be used to predict the biological nature of tissues. Clinical application of this technique began in early nineties with neuroimaging, mainly due to favourable MR characteristics and technical factors, but gradually its use has been extended to extracranial sites. Its application in head and neck lesions include characterization of cervical lymph nodes, salivary gland tumours, skull base lesions, differentiation of necrotic and viable parts of tumours with varying levels of success.

The basic principle of DWI is based on the fact that water molecules are always in random "Brownian" motion. This free movement is somewhat impeded in biological tissues due to interaction of water molecules with cell membranes and intracellular organelles. Benign tissues with relatively sparse cellularity and smaller nucleus to cytoplasmic ratio have sufficient space and allow relatively free mobility of water molecules[1]. This translates into facilitated diffusion on DWI. On the other hand, malignant tissues have densely packed cells which tend to have a larger nucleus occupying a relatively larger area of cytoplasm (higher nucleus to cytoplasmic ratio). As a result, malignant tissues offer more resistance to free movement of water molecules resulting in restricted diffusion.

However, while interpreting DWI in clinical practice; one needs to be aware of the fact that apart from tissue cellularity, tumours can have other histologic attributes including matrix composition which can have significant bearing on diffusion characteristics. Examples include fibrous tissues with extracellular collagen and lymphoid stroma which is known to show restricted diffusion[2]. In addition, some atypical entities despite being benign can have inherently increased cellularity and hence, can mimic malignant lesions on DWI. Prior knowledge of these lesions can reduce the possibility of potential misdiagnosis thereby, improving the diagnostic accuracy.

This article presents a spectrum of benign neck masses which show restricted pattern of diffusion and hence can lead to potential errors in diagnosis.

WARTHIN'S TUMOUR

Warthin's tumour (papillary cystadenoma lymphomatosum) is the second most common benign salivary gland neoplasm following pleomorphic adenoma. It constitutes about 4%-15% of all salivary gland neoplasms[3]. It commonly presents as slow-growing painless masses in middle-aged men, occurring almost exclusively in parotid gland mostly involving the lower portion over the angle of mandible[4]. Bilaterality and multicentricity are frequently observed in this group of tumors.

Histologically, it is an adenoma containing both solid and cystic areas. The cysts are lined by papillary projections containing oncocytic epithelial cells, while the supporting stroma contains abundant lymphoid tissue with lymphoid follicles and germinal centres[5] (Figure 1). These tumors have also been shown to have the highest microvessel count of all the parotid gland tumours[6].

The appearance of Warthin's tumour on DWI has been well documented in literature. Despite a wide range of reported mean apparent diffusion coefficient (ADC) values ranging from 0.72 to 0.96 × 10^{-3} mm^2/s, the presence of restricted diffusion has been reported uniformly in this entity[7-10] (Figure 1). Motoori *et al*[11] have in fact, reported an overlap of mean ADC values with those of malignant salivary gland tumors, especially salivary duct carcinoma. The proposed reason for such an appearance is the presence of predominant lymphoid stroma along with cysts containing thick proteinaceous content which inhibit free movement of water molecules[5]. Hence one needs to be aware of this entity and not to depend solely on DWI for characterization of parotid gland lesions.

NERVE SHEATH TUMOUR

Benign nerve sheath tumours are common in head and neck region accounting for about 25%-45% of all locations[12]. Histologically, they belong to two distinct groups namely schwannoma and neurofibroma, with the former being more common. Anatomically, parapharyngeal space is the most common location of nerve sheath tumours. Majority arise from the vagus nerve followed by cervical sympathetic chain and glossopharyngeal nerve. They mostly present as slow-growing, painless masses and hence, are late to come to clinical attention.

Schwannomas are known to have a heterogeneous appearance due to high propensity of cystic degeneration, xanthomatous changes and microhemorrhages[13] (Figure 2). Two distinct patterns of cellular arrangement are noted in schwannoma: Antoni A and Antoni B. Antoni A areas are highly cellular and composed of compact stacked arrangement of elongated cells. Alternating with these are relatively hypocellular Antoni B areas which contain loosely spaced cells with intervening microcystic spaces filled with mucin[14] (Figure 2).

Diffusion characteristics of schwannoms are not well documented in literature. Sener[15] reported facilitated diffusion in their series of six solid vestibular schwannoma while, isolated case reports have mentioned restricted diffusion in benign schwannomas. However, all the studies mention variable diffusion characteristics with a wide range of mean ADC values[16-20]. From a histological point of view, presence of areas of relative hypocellularity adjacent to either hypercellular or collagenous areas can probably explain the regional

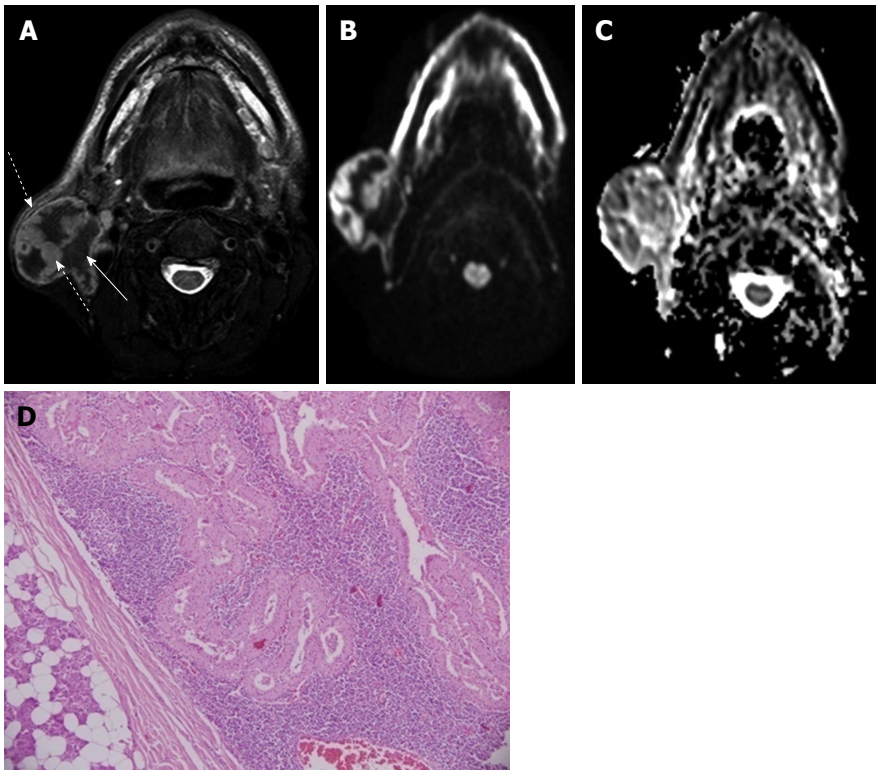

Figure 1 Warthin's tumour in right parotid gland in a 60-year-old man. A: Axial T2W FS image shows heterogeneous solid-cystic mass arising exophytically from right parotid gland with mildly hyperintense septae and mural nodules (dashed arrow) while cystic areas are hypointense (solid arrow); B and C: DWI at b1000 (B) s/mm² and ADC map (C) show restricted diffusion in septae and mural nodules of the mass; D: Photomicrograph shows a well encapsulated tumor comprising of acini with oncocytic change separated by sheets of lymphocytes (H-E; original magnification: × 100). DWI: Diffusion weighted imaging; ADC: Apparent diffusion coefficient.

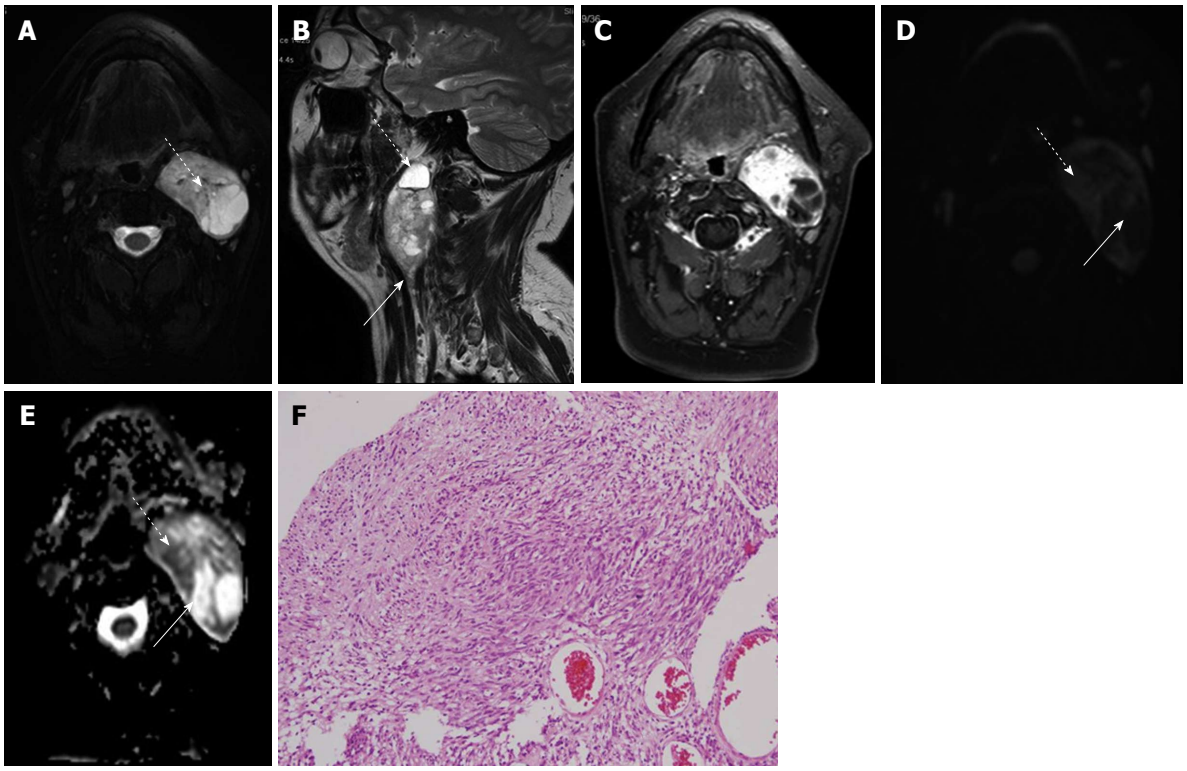

Figure 2 Left parapharyngeal space nerve sheath tumour in a 35-year-old lady. A: Axial T2W FS image shows multiple intensely T2 hyperintense areas within suggestive of cystic degeneration (dashed arrow); B: Sagittal T2W image shows blood fluid level within the cystic areas (dashed arrow) along with thickened distal exiting nerve (solid arrow); C: Axial T1W FS post contrast image shows intense enhancement in solid areas of the mass while cystic areas are hypointense; D and E: DWI at b1000 (D) s/mm² and ADC map (E) show restricted diffusion in solid areas of the mass (dashed arrow) while cystic areas show free diffusion (solid arrows); F: Photomicrograph shows alternating hypercellular (Antoni A) and hypocellular (Antoni B) areas (H-E; original magnification: × 100). DWI: Diffusion weighted imaging; ADC: Apparent diffusion coefficient.

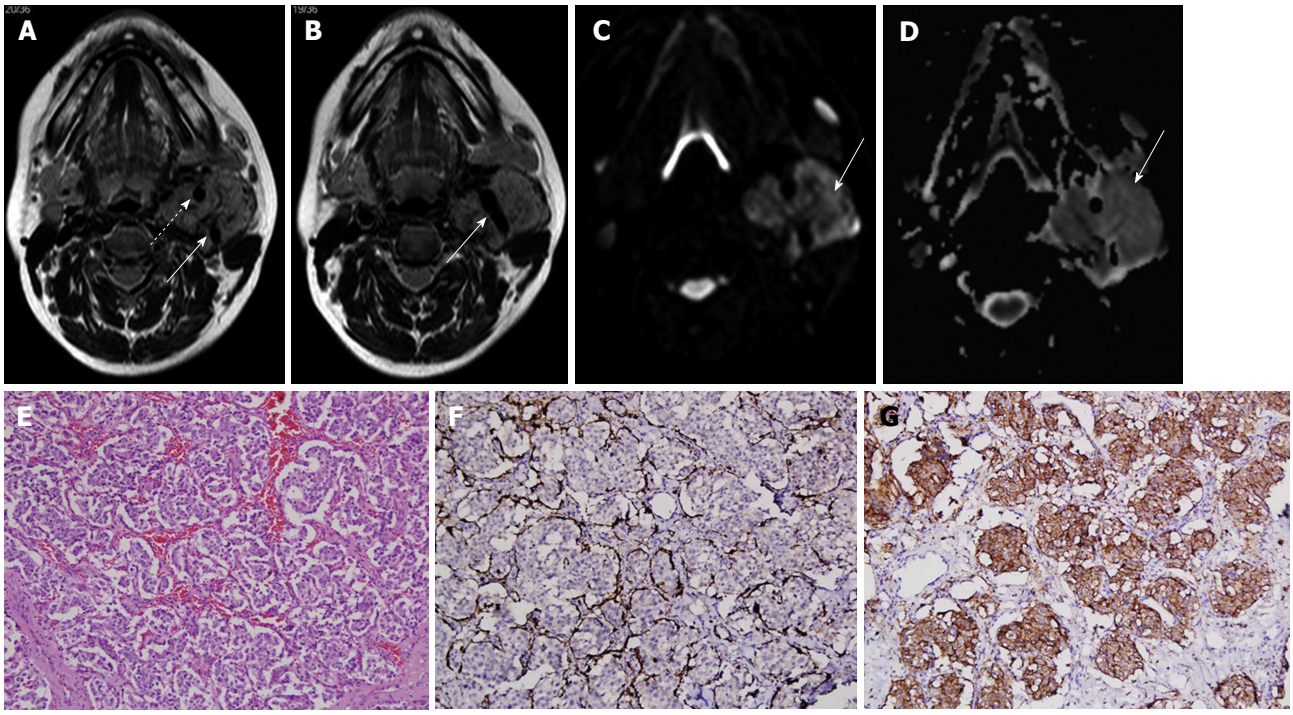

Figure 3 Carotid body tumour in a 30-year-old lady. A and B: Axial T2W images show heterogeneously hyperintense mass in left carotid space splaying the bifurcation of left common carotid artery (arrow in B) with encasement of both ECA and ICA (dashed arrow and solid arrow in A, respectively); C and D: DWI at b500 s/mm² (C) and ADC map (D) show restricted diffusion in the mass; E: Photomicrographs show tumor cells arranged in Zellballen pattern separated by thin fibrovascular septae (H-E; original magnification: × 200); F and G: S-100 immunostain demonstrating prominence of sustentacular cells at the periphery of the tumor cell nests (F, original magnification, × 200) and tumor cells are immunopositive for synaptophysin (G, original magnification: × 200). DWI: Diffusion weighted imaging; ADC: Apparent diffusion coefficient; ECA: External carotid artery; ICA: Internal carotid artery.

variation of diffusion characteristics in the same lesion. Peripheral areas of restriction likely correspond to hypercellular areas or areas with dense fibrous stroma while central areas of free diffusion correspond to hypocellular or cystic areas (Figure 2).

PARAGANGLIOMA

Paragangliomas are tumours of neural crest origin that occur along the distribution of these cells in specific locations of body. In head and neck, four common locations are observed: Carotid body at bifurcation of common carotid artery, jugular foramen, along the course of vagus nerve and middle ear cavity. Other less common locations include sella turcica[21], pineal gland, cavernous sinus and orbit. They comprise about 0.6% all tumours of head and neck[22]. Paraganglioma occurring in the neck produce characteristic displacement of adjacent vessels which help in their identification. Carotid body tumour splays the bifurcation of common carotid artery, encasing external carotid artery (ECA) and internal carotid artery (ICA) as it grows. However, the vessel lumen is usually not compromised[23] (Figure 3). Paraganglioma arising along the course of vagus nerve usually arise either from the superior ganglion (jugular ganglion) which is close to jugular foramen or from inferior ganglion (nodose ganglion). When arising from inferior ganglion, they produce anteromedial displacement of carotid vessels and posterolateral displacement of internal jugular vein, without any splaying of ECA and ICA.

Histologically, these tumours show a biphasic pattern composed of chief cells and supporting sustentacular cells with a fibrovascular stroma. The chief cells are more numerous and are compactly organized into cell rests known as zellballen pattern. The chief cells occupy central position in these clusters surrounded peripherally by sustentacular cells which characteristically have long cytoplasmic processes. This arrangement gives an overall whorled configuration to the cell clusters. The background stroma shows varying degree of hyalinization which tends to be higher in carotid body tumour. Immunohistochemical techniques can detect specific markers elicited by chief and sustentacular cells which includes chromagranin (present in neurosecretory granules of chief cells) and S-100 (sustentacular cell marker) and are widely used for diagnosis[23] (Figure 3).

The DWI appearance of paragangliomas has not been well documented in literature. Aschenbach *et al*[24] in their study of skull base lesions evaluated seven paragangliomas and found a mean ADC value of 1.304 ± 0.257 × 10^{-3} mm^2/s which was significantly different from other jugular fossa lesions. Others have reported hyperintense signal in urinary bladder paragangliomas on DWI, implying restricted diffusion[25]. DWI has also been used to differentiate between benign and malignant paragangliomas with the latter showing significantly lower mean ADC values than the former (0.918 ± 0.124) × 10^{-3} mm^2/s *vs* (1.175 ± 0.132) × 10^{-3} mm^2/s[26].

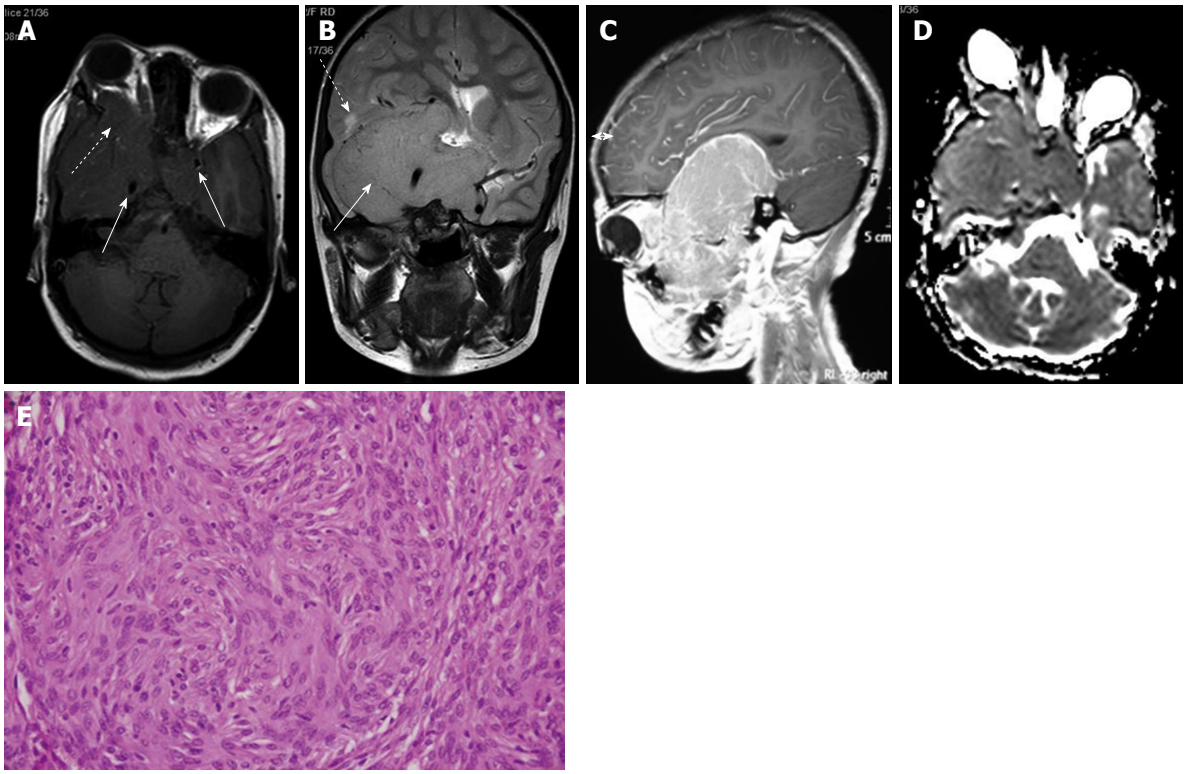

Figure 4 Craniofacial meningioma in a 7-year-old girl. A: Axial T1W image shows isointense homogenous mass involving bilateral cavernous sinuses (solid arrows) encasing bilateral ICAs and extending to right orbit causing proptosis (dashed arrow); B: Coronal T2W image shows intracranial extension in right middle cranial fossa (solid arrow) with mild perilesional edema in adjacent cerebral parenchyma (dashed arrow); C: Sagittal T1W FS post-gadolinium image reveals intense homogeneous enhancement in the mass; D: ADC map showing homogenous restricted diffusion in the mass; E: Photomicrograph show tumour composed of spindled to polygonal cells with moderate amount of cytoplasm, vesicular nuclei and whorl formation at places (H-E; original magnification: × 400). ADC: Apparent diffusion coefficient; ICA: Internal carotid artery.

Such atypical behavior of paragangliomas on DWI can be explained to some extent, by the compact histological arrangement of its constituent cells. These tumours show whorled arrangement of cells with presence of variable amount of collagen deposition in their stroma which leaves little extracellular space for free movement of water molecules (Figure 3). This hypothesis can be extrapolated to explain the lower ADC observed in malignant pheochromocytomas with increased cellularity and reduced extracellular space compared to their benign counterparts. However, a definite histological explanation warrants large scale studies to validate these findings.

MENINGIOMA

Primary extracranial meningiomas are rare tumours (< 2%) and their most common location includes head and neck especially sinonasal region, ear, temporal bone and scalp[27]. Their origin is hypothesized to be from arachnoidal cells which tend to migrate outside the neuraxis producing extracranial meningiomas. In about 20% cases, extracranial meningiomas have an intracranial extension. These tumors have a female preponderance which can be attributed to presence of progesterone-dependent growth[28].

Histologically, meningiomas are made up of whorls of neoplastic epitheloid cells with indistinct borders (Figure 4). They frequently show psammoma bodies and intranuclear pseudo-inclusions[27,29]. In addition, various histologic subtypes have been identified including meningothelial, fibrous, angiomatous, transitional, psammomatous or atypical. Increased collagen formation has been noted in meningiomas irrespective of tumour grade which has been attributed to presence of meningiothelial cells[28]. Such fibrous stroma coupled with heterogeneous histologic composition leads to variable diffusion characteristics.

There are limited studies documenting the role of DWI in meningiomas. While the major emphasis has been on differentiation of benign and atypical/malignant meningiomas using mean and normalized ADC values, the variable nature of diffusion characteristics in benign meningiomas has also been mentioned[30-32] (Figure 4).

Hakyemez *et al*[32] have reported different ranges of mean ADC values in different subtypes of benign meningiomas. Others have also mentioned variable signal intensity of benign meningiomas on DWI with malignant/atypical meningiomas showing relative restriction compared to their benign counterparts[31].

SOLITARY FIBROUS TUMOUR

Solitary fibrous tumour (SFT) is a rare neoplasm of mesenchymal origin[33]. Although, most frequently seen

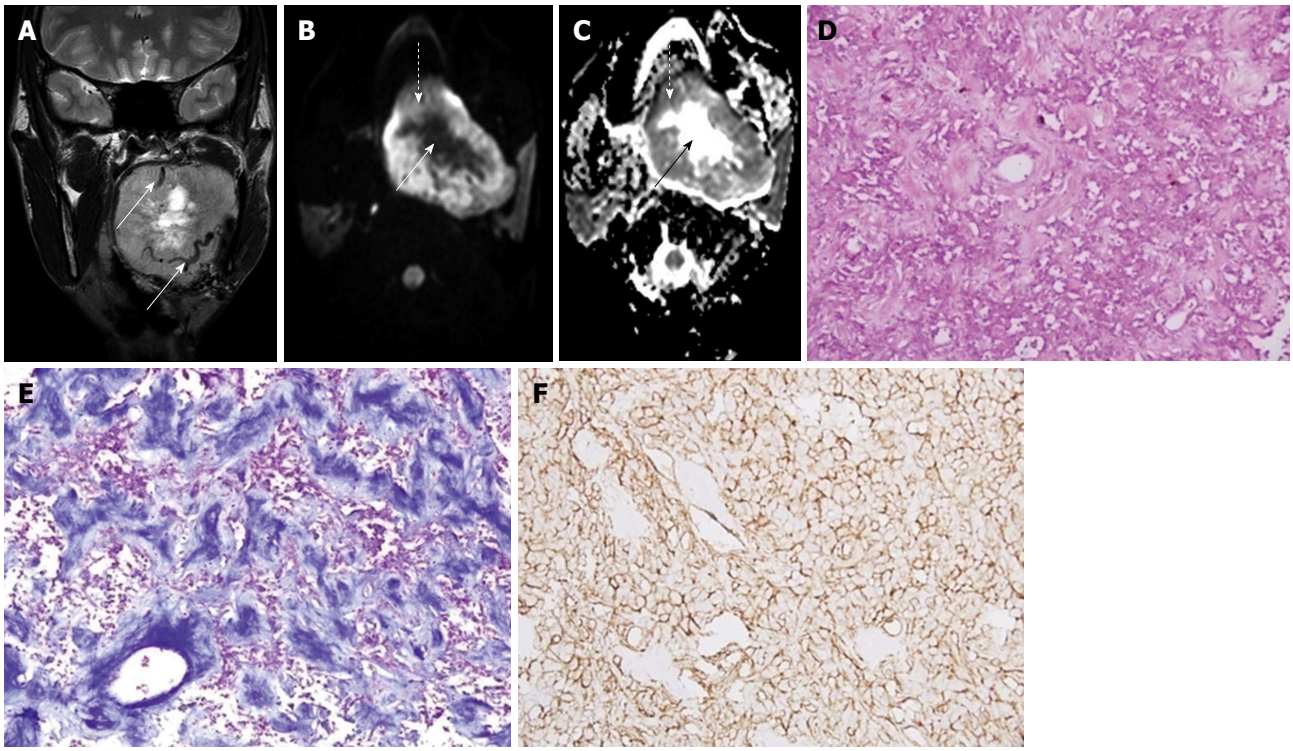

Figure 5 Solitary fibrous tumour in a 24-year-old man. A: Coronal T2W image shows well defined left parapharyngeal space mass with heterogeneously hyperintense signal. The core is more hyperintense than the periphery. Multiple tortuous flow voids seen in the mass (solid arrows); B and C: DWI at b1000 (B) s/mm² and corresponding ADC map (C) show restricted diffusion in the periphery of the mass (dashed arrows) while the centre shows free diffusion (solid arrow); D: Photomicrographs show alternating cellular and hypocellular areas with abundant collagen (H-E; original magnification: × 200); E and F: Masson trichrome stain highlighting abundant collagen (E; original magnification: × 200); tumor cells are diffusely immunopositive for CD34 (F; original magnification: × 400). DWI: Diffusion weighted imaging; ADC: Apparent diffusion coefficient.

to arise from pleura, occasional SFTs have been documented at various extra-pleural sites including lung, mediastinum, pericardium, liver and head and neck. Extracranial head and neck SFTs have been reported in oral cavity, paranasal sinuses, orbit, nasal cavity and parapharyngeal space. Most of these tumours are benign with complete surgical excision being the treatment of choice.

Histologically, they are well circumscribed masses predominantly populated by spindle cells with abundant extracellular collagen. Distinct immunohistochemical features characterize these tumours which include diffuse CD34 positivity and epithelial membrane antigen negativity[34] (Figure 5). Some tumours may show hypocellular areas with profuse extra-cellular collagen deposition alternating with hypercellular areas[35].

MRI reveals heterogeneous appearance of SFTs on T2 weighted images. They show focal areas of relative T2 hypointensity interspersed with hyperintense areas which corresponds to hypocellular collagenous areas and hypercellular areas respectively. These contrasting signal intensities on T2 weighted images produce the so called "yin-yang" appearance[36]. These tumours are usually hypervascular with frequent presence of vascular flow voids[37]. Diffusion weighted imaging shows areas of restricted diffusion in some parts of these lesions which has been attributed to the presence of focal areas of hypercellularity in them[36,38] (Figure 5).

HEMANGIOPERICYTOMA

Hemangiopericytoma (HPC) is a rare mesenchymal neoplasm originating from Zimmermann pericytes which are modified smooth muscle cells outlining capillaries and post-capillary venules[39]. Although any age group can be affected, they are most frequently seen in fifth and sixth decades[40]. About 15%-30% of them occur in head and neck which is the third most common site following lower extremities and retroperitoneum-pelvis, respectively[41]. Tumours in head and neck commonly arise in the neck, perioral soft tissue and sinonasal tract[41]. Sinonasal HPCs are believed to have less aggressive biological behaviour compared to their peripheral counterparts. Complete surgical excision with negative margins is the treatment of choice.

HPCs belong to the same histological spectrum as SFTs with common imaging and clinical features. They are hypercellular and vascular lesions with compact arrangement of cells containing scant cytoplasm (Figure 6). Dilated vessels are interspersed showing a branching pattern resembling "staghorn" appearance[42].

DWI has been used to differentiate intracranial HPCs from meningiomas based on significantly lower minADC values in meningiomas as compared to HPCs ($0.875 \pm 0.014 \times 10^{-3}$ mm²/s and $1.116 \pm 0.127 \times 10^{-3}$ mm²/s, respectively)[43]. The possible explanation being offered is a relatively lower cellularity and prominent vascularity

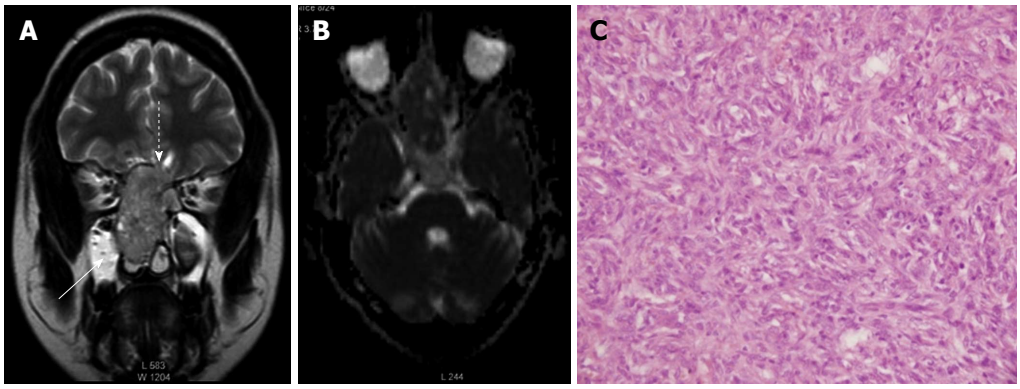

Figure 6 Sinonasal hemangiopericytoma in a 45-year-old lady. A: Coronal T2W image shows mildly expansile sinonasal mass involving, extending to bilateral ethmoid sinuses. Small intracranial extension noted in anterior cranial fossa (dashed arrow); Retained secretions in right maxillary sinus (solid arrow); B: ADC map shows restricted diffusion in the mass; C: Photomicrograph shows spindle cells with mild pleomorphism (H-E; original magnification: × 100). ADC: Apparent diffusion coefficient.

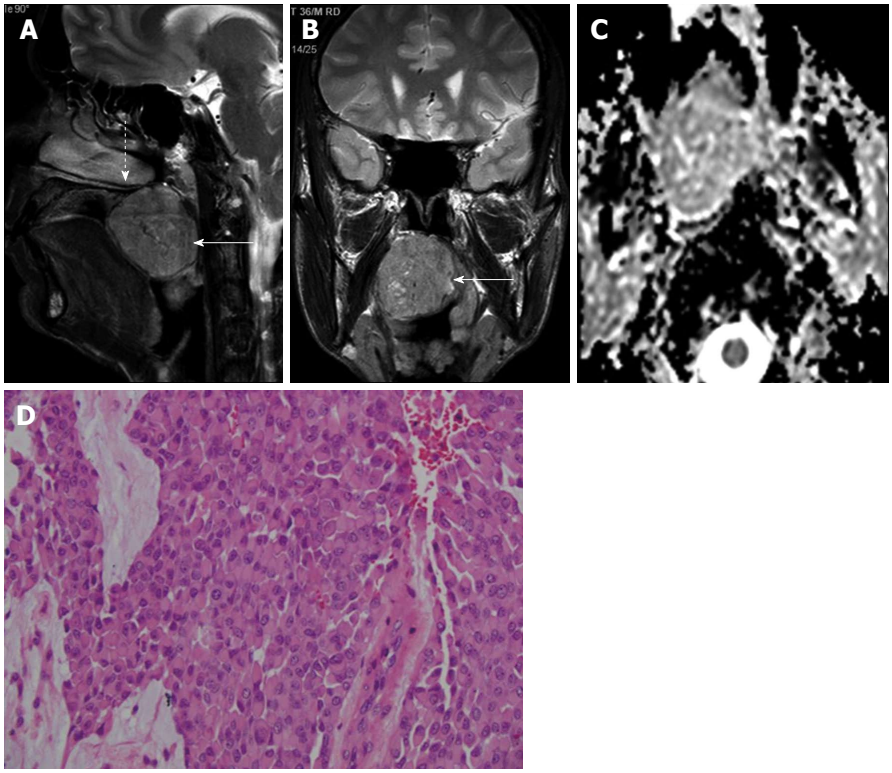

Figure 7 Myoepithelial tumour in a 36-year-old man. A and B: Sagittal T2W image shows well defined T2 hyperintense mass arising from posterior part of soft palate (dashed arrow in A and B) and into the oropharynx (solid arrow in A and B); C: ADC map shows restricted diffusion in the mass; D: Photomicrograph shows cells with abundant cytoplasm and minimal pleomorphism (H-E; original magnification: × 100).

in HPCs as compared to meningiomas. However, owing to the inherently hypercellular tumour matrix of HPCs, free movement of water molecules is hindered producing a qualitative pattern of restricted diffusion (Figure 6).

MYOEPITHELIAL TUMOUR

Myoepithelial tumours are rare benign neoplasms constituting about 1%-1.5% of salivary tumours. About 40% of them occur in parotid glands followed by submandibular glands and minor salivary glands; most common location being the palate[44,45] (Figure 7). They belong to the same histological spectrum as pleomorphic adenoma but are more aggressive. However, World Health Organization has recognized it as a separate entity showing less than 5% or no ductal and acinar differentiation, which are present in pleomorphic adenoma[45].

Histologically, myoepithelial tumours can be composed of spindle-shaped, plasmacytoid, epitheloid or clear cells in varying proportions. The growth pattern can appear as solid (non-myxoid), reticular or mixed type[46]. Histological subtype is related to the location of these tumours. Plasmacytoid type occurs more commonly in

Table 1 Space-wise distribution of benign entities showing restricted diffusion in head and neck

Neck space	Benign entities with restricted diffusion
Parapharyngeal space	Nerve sheath tumour
Carotid space	Paraganglioma
	Nerve sheath tumour
Parotid space	Warthin's tumour
	Myoepithelial tumour
Oral cavity	Myoepithelial tumour
Sinonasal cavity	Meningioma
	Hemangiopericytoma
	Solitary fibrous tumour
Ear/temporal bone	Paraganglioma (glomus tympanicum)
	Meningioma
	Nerve sheath tumour
Miscellaneous	Nerve sheath tumour
	Hemangiopericytoma
	Solitary fibrous tumour

minor salivary glands of oral cavity, while spindle-cell and clear cell type are more often seen in parotid glands[47]. The background stroma is composed of variable amount of fibro-collagenous or myxoid stroma.

The MR imaging appearance of myoepithelial tumours has sporadically been reported in literature. They are isointense on T1 weighted image and intensely hyperintense on T2 weighted images with homogenous contrast enhancement. However, their behavior on DWI has not been documented earlier. We have observed hyperintense signal on DWI in myoepithelial tumour which can possibly be attributed to its plasmacytoid histology characterized by closely packed arrangement of neoplastic cells (Figure 7). However, keeping in view the variable histological make-up of these tumours, they can have variable appearance on DWI. Further studies are therefore, needed to validate these findings.

DWI has long been used successfully for diagnosis and characterization of lesions as benign and malignant; there are few atypical entities which do not conform to the expected behavior according to their biological nature. While some of these entities occur in specific neck spaces, others are more non-specific in their distribution (Table 1). A knowledge of these exceptions and their preferred distribution in various neck spaces helps to narrow the possible list of differential diagnoses and avoid possible errors in diagnosis.

REFERENCES

1 **Wang J**, Takashima S, Takayama F, Kawakami S, Saito A, Matsushita T, Momose M, Ishiyama T. Head and neck lesions: characterization with diffusion-weighted echo-planar MR imaging. *Radiology* 2001; **220**: 621-630 [PMID: 11526259 DOI: 10.1148/radiol.2202010063]

2 **Qayyum A**. Diffusion-weighted imaging in the abdomen and pelvis: concepts and applications. *Radiographics* 2009; **29**: 1797-1810 [PMID: 19959522 DOI: 10.1148/rg.296095521]

3 **Som PM**, Brandwein MS. Salivary glands: anatomy and pathology. In: Som PM, Curtin HD, editors. Head and neck imaging. 4th ed. St. Louis, Mo: Mosby, 2003: 2005-2133

4 **Eveson JW**, Cawson RA. Salivary gland tumours. A review of 2410 cases with particular reference to histological types, site, age and sex distribution. *J Pathol* 1985; **146**: 51-58 [PMID: 4009321 DOI: 10.1002/path.1711460106]

5 **Ikeda M**, Motoori K, Hanazawa T, Nagai Y, Yamamoto S, Ueda T, Funatsu H, Ito H. Warthin tumor of the parotid gland: diagnostic value of MR imaging with histopathologic correlation. *AJNR Am J Neuroradiol* 2004; **25**: 1256-1262 [PMID: 15313720]

6 **Yabuuchi H**, Fukuya T, Tajima T, Hachitanda Y, Tomita K, Koga M. Salivary gland tumors: diagnostic value of gadolinium-enhanced dynamic MR imaging with histopathologic correlation. *Radiology* 2003; **226**: 345-354 [PMID: 12563124 DOI: 10.1148/radiol.2262011486]

7 **Habermann CR**, Gossrau P, Graessner J, Arndt C, Cramer MC, Reitmeier F, Jaehne M, Adam G. Diffusion-weighted echo-planar MRI: a valuable tool for differentiating primary parotid gland tumors? *Rofo* 2005; **177**: 940-945 [PMID: 15973595 DOI: 10.1055/s-2005-858297]

8 **Yoshino N**, Yamada I, Ohbayashi N, Honda E, Ida M, Kurabayashi T, Maruyama K, Sasaki T. Salivary glands and lesions: evaluation of apparent diffusion coefficients with split-echo diffusion-weighted MR imaging--initial results. *Radiology* 2001; **221**: 837-842 [PMID: 11719687 DOI: 10.1148/radiol.2213010131]

9 **Habermann CR**, Arndt C, Graessner J, Diestel L, Petersen KU, Reitmeier F, Ussmueller JO, Adam G, Jaehne M. Diffusion-weighted echo-planar MR imaging of primary parotid gland tumors: is a prediction of different histologic subtypes possible? *AJNR Am J Neuroradiol* 2009; **30**: 591-596 [PMID: 19131405 DOI: 10.3174/ajnr.A1412]

10 **Şerifoğlu İ**, Oz İİ, Damar M, Tokgöz Ö, Yazgan Ö, Erdem Z. Diffusion-weighted imaging in the head and neck region: usefulness of apparent diffusion coefficient values for characterization of lesions. *Diagn Interv Radiol* 2015; **21**: 208-214 [PMID: 25910284 DOI: 10.5152/dir.2014.14279]

11 **Motoori K**, Iida Y, Nagai Y, Yamamoto S, Ueda T, Funatsu H, Ito H, Yoshitaka O. MR imaging of salivary duct carcinoma. *AJNR Am J Neuroradiol* 2005; **26**: 1201-1206 [PMID: 15891184]

12 **Colreavy MP**, Lacy PD, Hughes J, Bouchier-Hayes D, Brennan P, O'Dwyer AJ, Donnelly MJ, Gaffney R, Maguire A, O'Dwyer TP, Timon CV, Walsh MA. Head and neck schwannomas--a 10 year review. *J Laryngol Otol* 2000; **114**: 119-124 [PMID: 10748827 DOI: 10.1258/0022215001905058]

13 **Cohen LM**, Schwartz AM, Rockoff SD. Benign schwannomas: pathologic basis for CT inhomogeneities. *AJR Am J Roentgenol* 1986; **147**: 141-143 [PMID: 3487205 DOI: 10.2214/ajr.147.1.141]

14 **McLendon RE**, Bigner DD, Bigner SH. Intracranial and intraspinal schwannomas (WHO grade I). In: Pathology of Tumors of the Central Nervous System: A Guide to Histologic Diagnosis. London: Arnold; 2000: 71-81

15 **Sener RN**. Diffusion magnetic resonance imaging of solid vestibular schwannomas. *J Comput Assist Tomogr* 2003; **27**: 249-252 [PMID: 12703020 DOI: 10.1097/00004728-200301000-00007]

16 **Srinivasan A**, Dvorak R, Perni K, Rohrer S, Mukherji SK. Differentiation of benign and malignant pathology in the head and neck using 3T apparent diffusion coefficient values: early experience. *AJNR Am J Neuroradiol* 2008; **29**: 40-44 [PMID: 17921228 DOI: 10.3174/ajnr.A0743]

17 **Khedr SA**, Hassan MA, Abdelrazek NM, Sakr Ay. Diagnostic impact of echo planar diffusion-weighted magnetic resonance imaging (DWI) in musculoskeletal neoplastic masses using apparent diffusion coefficient (ADC) mapping as a quantitative assessment tool. *Egyptian J Radiol Nuc Med* 2012; **43**: 249-256 [DOI: 10.1016/j.ejrnm.2012.01.003]

18 **Fayad LM**, Blakeley J, Plotkin S, Widemann B, Jacobs MA. Whole Body MRI at 3T with Quantitative Diffusion Weighted Imaging and Contrast-Enhanced Sequences for the Characterization of Peripheral Lesions in Patients with Neurofibromatosis Type 2 and Schwannomatosis. *ISRN Radiol* 2013; **2013**: 9 [DOI: 10.5402/2013/627932]

19 **Chhabra A**, Thakkar RS, Andreisek G, Chalian M, Belzberg AJ,

Blakeley J, Hoke A, Thawait GK, Eng J, Carrino JA. Anatomic MR imaging and functional diffusion tensor imaging of peripheral nerve tumors and tumorlike conditions. *AJNR Am J Neuroradiol* 2013; **34**: 802-807 [PMID: 23124644 DOI: 10.3174/ajnr.A3316]

20 **Sumi M**, Nakamura T. Head and neck tumours: combined MRI assessment based on IVIM and TIC analyses for the differentiation of tumors of different histological types. *Eur Radiol* 2014; **24**: 223-231 [PMID: 24013848 DOI: 10.1007/s00330-013-3002-z]

21 **Noble ER**, Smoker WR, Ghatak NR. Atypical skull base paragangliomas. *AJNR Am J Neuroradiol* 1997; **18**: 986-990 [PMID: 9159383]

22 **Borba LA**, Al-Mefty O. Intravagal paragangliomas: report of four cases. *Neurosurgery* 1996; **38**: 569-575; discussion 575 [PMID: 8837811 DOI: 10.1227/00006123-199603000-00030]

23 **Rao AB**, Koeller KK, Adair CF. From the archives of the AFIP. Paragangliomas of the head and neck: radiologic-pathologic correlation. Armed Forces Institute of Pathology. *Radiographics* 1999; **19**: 1605-1632 [PMID: 10555678]

24 **Aschenbach R**, Basche S, Vogl TJ, Klisch J. Diffusion-weighted imaging and ADC mapping of head-and-neck paragangliomas: initial experience. *Klin Neuroradiol* 2009; **19**: 215-219 [PMID: 19705076 DOI: 10.1007/s00062-009-9004-1]

25 **Wang H**, Ye H, Guo A, Wei Z, Zhang X, Zhong Y, Fan Z, Wang Y, Wang D. Bladder paraganglioma in adults: MR appearance in four patients. *Eur J Radiol* 2011; **80**: e217-e220 [PMID: 20950973 DOI: 10.1016/j.ejrad.2010.09.020]

26 **Dong Y**, Liu Q. Differentiation of malignant from benign pheochromocytomas with diffusion-weighted and dynamic contrast-enhanced magnetic resonance at 3.0 T. *J Comput Assist Tomogr* 2012; **36**: 361-366 [PMID: 22805661 DOI: 10.1097/RCT.0b013e31825975f8]

27 **Rushing EJ**, Bouffard JP, McCall S, Olsen C, Mena H, Sandberg GD, Thompson LD. Primary extracranial meningiomas: an analysis of 146 cases. *Head Neck Pathol* 2009; **3**: 116-130 [PMID: 19644540 DOI: 10.1007/s12105-009-0118-1]

28 **Backer-Grøndahl T**, Moen BH, Torp SH. The histopathological spectrum of human meningiomas. *Int J Clin Exp Pathol* 2012; **5**: 231-242 [PMID: 22558478]

29 **Thompson LD**, Gyure KA. Extracranial sinonasal tract meningiomas: a clinicopathologic study of 30 cases with a review of the literature. *Am J Surg Pathol* 2000; **24**: 640-650 [PMID: 10800982 DOI: 10.1097/00000478-200005000-00002]

30 **Nagar VA**, Ye JR, Ng WH, Chan YH, Hui F, Lee CK, Lim CC. Diffusion-weighted MR imaging: diagnosing atypical or malignant meningiomas and detecting tumor dedifferentiation. *AJNR Am J Neuroradiol* 2008; **29**: 1147-1152 [PMID: 18356472 DOI: 10.3174/ajnr.A0996]

31 **Filippi CG**, Edgar MA, Uluğ AM, Prowda JC, Heier LA, Zimmerman RD. Appearance of meningiomas on diffusion-weighted images: correlating diffusion constants with histopathologic findings. *AJNR Am J Neuroradiol* 2001; **22**: 65-72 [PMID: 11158890]

32 **Hakyemez B**, Yildirim N, Erdoğan C, Kocaeli H, Korfali E, Parlak M. Meningiomas with conventional MRI findings resembling intraaxial tumors: can perfusion-weighted MRI be helpful in differentiation? *Neuroradiology* 2006; **48**: 695-702 [PMID: 16896907 DOI: 10.1007/s00234-006-0115-y]

33 **Goodlad JR**, Fletcher CD. Solitary fibrous tumour arising at unusual sites: analysis of a series. *Histopathology* 1991; **19**: 515-522 [PMID: 1786936 DOI: 10.1111/j.1365-2559.1991.tb01499.x]

34 **Mekni A**, Kourda J, Hammouda KB, Tangour M, Kchir N, Zitouna M, Haouet S. Solitary fibrous tumour of the central nervous system: pathological study of eight cases and review of the literature. *Pathology* 2009; **41**: 649-654 [PMID: 19672786 DOI: 10.3109/00313020903071439]

35 **Smith AB**, Horkanyne-Szakaly I, Schroeder JW, Rushing EJ. From the radiologic pathology archives: mass lesions of the dura: beyond meningioma-radiologic-pathologic correlation. *Radiographics* 2014; **34**: 295-312 [PMID: 24617680 DOI: 10.1148/rg.342130075]

36 **Kim HJ**, Lee HK, Seo JJ, Kim HJ, Shin JH, Jeong AK, Lee JH, Cho KJ. MR imaging of solitary fibrous tumors in the head and neck. *Korean J Radiol* 2005; **6**: 136-142 [PMID: 16145288 DOI: 10.3348/kjr.2005.6.3.136]

37 **Tateishi U**, Nishihara H, Morikawa T, Miyasaka K. Solitary fibrous tumor of the pleura: MR appearance and enhancement pattern. *J Comput Assist Tomogr* 2002; **26**: 174-179 [PMID: 11884769 DOI: 10.1097/00004728-200203000-00002]

38 **Clarençon F**, Bonneville F, Rousseau A, Galanaud D, Kujas M, Naggara O, Cornu P, Chiras J. Intracranial solitary fibrous tumor: imaging findings. *Eur J Radiol* 2011; **80**: 387-394 [PMID: 20303226 DOI: 10.1016/j.ejrad.2010.02.016]

39 **Stout AP**, Murray MR. Hemangiopericytoma: a vascular tumor featuring zimmermann's pericytes. *Ann Surg* 1942; **116**: 26-33 [PMID: 17858068 DOI: 10.1097/00000658-194207000-00004]

40 **McMaster MJ**, Soule EH, Ivins JC. Hemangiopericytoma. A clinicopathologic study and long-term followup of 60 patients. *Cancer* 1975; **36**: 2232-2244 [PMID: 1203874 DOI: 10.1002/cncr.2820360942]

41 **Enzinger FM**, Smith BH. Hemangiopericytoma. An analysis of 106 cases. *Hum Pathol* 1976; **7**: 61-82 [PMID: 1244311 DOI: 10.1016/S0046-8177(76)80006-8]

42 **Giannini C**, Rushing EJ, Hainfellner JA. Haemangiopericytoma. In: Louis DN, Ohagaki H, Wiestler OD, Cavanees WK, editors. WHO classifiation of tumours of the central nervous system. Lyon, France: IARC, 2007: 178-180

43 **Liu G**, Chen ZY, Ma L, Lou X, Li SJ, Wang YL. Intracranial hemangiopericytoma: MR imaging findings and diagnostic usefulness of minimum ADC values. *J Magn Reson Imaging* 2013; **38**: 1146-1151 [PMID: 23463687 DOI: 10.1002/jmri.24075]

44 **Ferri E**, Pavon I, Armato E, Cavaleri S, Capuzzo P, Ianniello F. Myoepithelioma of a minor salivary gland of the cheek: case report. *Acta Otorhinolaryngol Ital* 2006; **26**: 43-46 [PMID: 18383757]

45 **Cuadra Zelaya F**, Quezada Rivera D, Tapia Vazquez JL, Paez Valencia C, Gaitán Cepeda LA. Plasmacytoid myoepithelioma of the palate. Report of one case and review of the literature. *Med Oral Patol Oral Cir Bucal* 2007; **12**: E552-E555 [PMID: 18059237]

46 **Dardick I**. Myoepithelioma: definitions and diagnostic criteria. *Ultrastruct Pathol* 1995; **19**: 335-345 [PMID: 7483010 DOI: 10.3109/01913129509021906]

47 **Bakshi J**, Parida PK, Mahesha V, Radotra BD. Plasmacytoid myoepithelioma of palate: three rare cases and literature review. *J Laryngol Otol* 2007; **121**: e13 [PMID: 17640425 DOI: 10.1017/S002221510700000X]

P- Reviewer: Chow J **S- Editor**: Qiu S
L- Editor: A **E- Editor**: Liu SQ

Published by **Baishideng Publishing Group Inc**
8226 Regency Drive, Pleasanton, CA 94588, USA
Telephone: +1-925-223-8242
Fax: +1-925-223-8243
E-mail: bpgoffice@wjgnet.com
Help Desk: http://www.wjgnet.com/esps/helpdesk.aspx
http://www.wjgnet.com